Received: 16 September 2020 | Revised: 21 October 2020 | Accepted: 29 October 2020

DOI: 10.1002/btm2.10197

RESEARCH REPORT

BIOENGINEERING & TRANSLATIONAL MEDICINE

Engineered macrophage membrane-enveloped nanomedicine for ameliorating myocardial infarction in a mouse model

Yugang Xue[1] | Guangwei Zeng[2] | Jin Cheng[1] | Jianqiang Hu[1] | Mingming Zhang[1] | Yan Li[1]

[1]Department of Cardiology, Tangdu Hospital, Air force Military Medical University, Xi'an, Shaanxi, China

[2]Section 2, Department of Cardiology, Xi'An International Medical Center Hospital, Xi'an, Shaanxi, China

Correspondence
Yan Li, Department of Cardiology, Tangdu Hospital, Air force Military Medical University, Xinsi Road, Baqiao District, Xi'an 710000, Shaanxi, China.
Email: profleeyan@163.com

Funding information
National Natural Science Foundation of China, Grant/Award Number: 82000350

Abstract

Myocardial infarction (MI) is the serious condition causing lots of death over the world. Myocytes apoptosis, inflammation, and fibrosis are three important factors implicated in pathogenesis of MI. Targeting these three factors has been shown to ameliorate MI and rescue cardiac function. Previous studies have demonstrated that microRNA (miR) 199a-3p protect against MI. In this study, we prepare macrophage membrane coated nanoparticles (MMNPs) containing miR199a-3p. We evaluate the effects of these NPs on apoptosis and cell proliferation *in vitro* and the effects on inflammation cytokine production, expression of fibrosis related proteins, cardiac injuries, and functions in MI mice. We find that the MMNPs have receptors of interleukin-1β (IL-1β), interleukin-6 (IL-6), and tumor necrosis factor alpha (TNF-α) and can bind to these cytokines. MMNPs prevent hypoxia-induced apoptosis and promote cell proliferation, suppress the inflammation, and inhibit the cardiac fibrosis in MI mice. These results demonstrate that MMNPs ameliorate left ventricular remodeling and cardiac functions, and protect against MI, suggesting MMNPs containing miR199a-3p is a potential therapeutic approach to treat MI.

KEYWORDS

macrophage membrane, mice, myocardial infarction, nanomedicine

1 | INTRODUCTION

Myocardial infarction (MI), also known as heart attack, is caused by decreased or stopped blood flow to the heart.[1] MI causes injuries to the heart muscle. Because of cardiomyocytes loss, MI damages myocardial functions and finally results in heart failure, causing major death and disability worldwide.

Apoptosis and fibrosis play essential roles in MI-induced tissue injury.[2] Following a MI, numerous cells die in response to ischemia. Apoptosis greatly contributes to myocytes death in MI and mostly occurs in the peri-infarcted region. Apoptosis plays a critical role in determining infarct size and early symptoms of heart failure.[3] Inhibition of apoptosis has been shown to improve cardiac functions and decrease infarct size in MI mice model.[4] Due to the limited capacity of heart regeneration, fibrotic scars replace the lost cells.[5] Fibrosis is an essential process for damage repair but the accumulation of fibrosis in tissues will lead to organ dysfunction and organ failure. Although inhibiting cardiac fibrosis from progressing has been recognized as important to prevent heart failure, there is still no efficient therapy available.

Inflammation is another hallmark of MI.[6] MI triggers inflammatory responses, which result in cytokine production and inflammatory leukocytes infiltration into myocardial region. After MI, elaborated cytokines have been identified in infarcted area. Elevated tumor necrosis

factor alpha (TNF-α), interleukin (IL)-1, and IL-6 have been shown to contribute to myocytes death, myocardial injury, and healing process.[6,7] Blockage of TNF-α, IL-1, and IL-6 has been shown to preserve the cardiac function, indicating targeting these inflammatory cytokines should be a potential therapeutic approach to treat MI.[8-11]

MicroRNAs (miRNAs) are short non-coding RNAs, which regulate gene expression. MiRNAs are shown to regulate various aspects of cardiomyocyte biology.[12] MiR-199a-3p has been shown to reduce the infarct size and improve cardiac function in MI mice.[13,14] Nanoparticles (NPs) have been utilized as novel approach to deliver drugs for multiple diseases treatments with higher specificity and fewer side effects. Cationic lipid-assisted PEG-b-PLGA nanoparticles (CLAN), which form a clinically translatable nucleic acid delivery system, has been also widely utilized to deliver miRNA, and these NPs containing miRNA have been shown to prevent cell apoptosis and improve myocardial remodeling after MI.[15] Recently, cell-membrane-enveloped NPs have been recognized as an encouraging therapeutic platform.[16] These NPs are fused with natural cell membranes and can absorb and neutralize molecules.[17,18] The neutrophil membrane-coated NPs have been described to neutralize pro-inflammatory cytokines, suppress inflammation, and against joint damage.[19] Taken together, the membrane coated NPs containing miRNA could be an efficient treatment for MI.

In the present study, we prepared NPs enveloped with membranes from engineered macrophages, which overexpressed TNF-αR, IL-1βR, and IL-6R. The NPs contained miR199a-3p, which has been shown to induce cardiomyocyte proliferation.[20] We investigated the potential effects of these membrane envelope NPs on cell proliferation, inflammatory response, and cardiac function in MI.

2 | RESULTS

2.1 | Preparation and characterization of macrophage membrane-enveloped NPs encapsulating miRNA

First, we prepared the engineered macrophage membrane-enveloped NPs encapsulating miR-199a-3p (Figure 1a). This nanoparticle was termed as MMNPmiR$_{199a-3p}$. The NPs encapsulating miR-199a-3p was denoted as NP$_{miR-199a-3p}$. The engineered macrophages had enhanced surface expression of IL-1βR, IL-6R, and TNF-αR (Figure 1b).

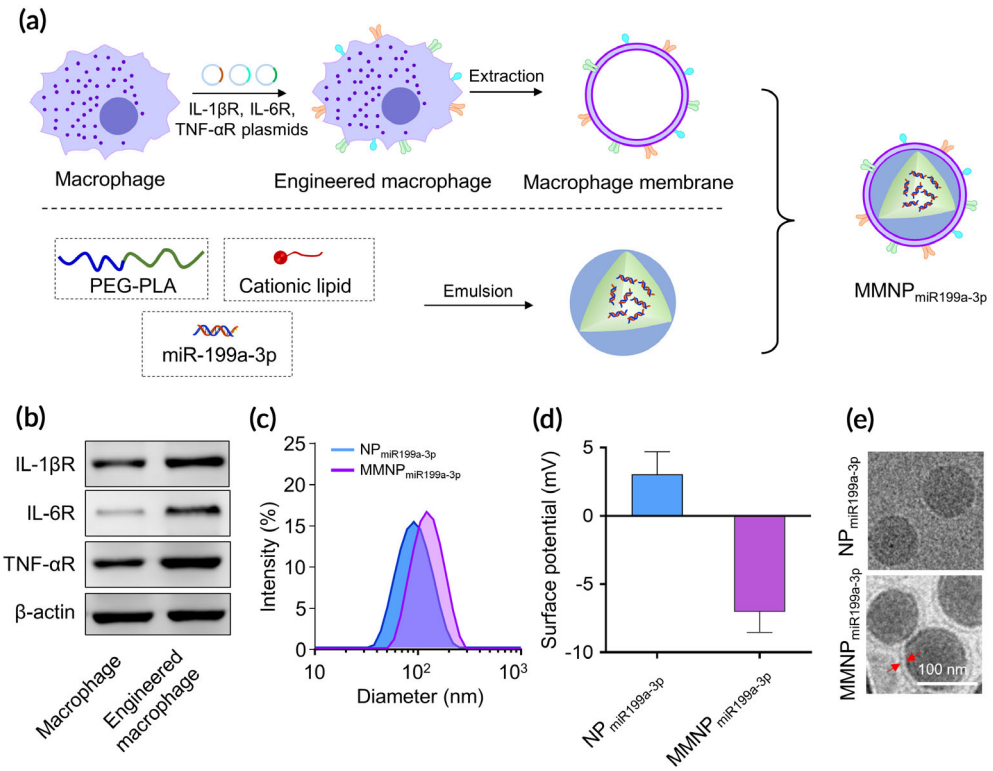

FIGURE 1 Construction of engineered macrophage membrane-enveloped nanoparticles encapsulating miR199a-3p for the amelioration of myocardial infarction. (a) Schematic representation of engineered macrophage membrane-enveloped nanoparticles encapsulating miR199a-3p. Murine macrophages were transfected with plasmids encoding IL-1βR, IL-6R, and TNF-αR. MiR199a-3p was encapsulated into polyethylene glycol–polylactic acid (PEG–PLA) via a double emulsion method, denoted as NP$_{miR199a-3p}$. Engineered macrophage membrane enveloped NPmiR199a-3p was denoted as MMNP$_{miR199a-3p}$. The hydrodynamic size (b) and zeta potential (c) of NP$_{miR199a-3p}$ and MMNP$_{miR199a-3p}$ were examined dynamic light scattering (DLS). (d) Representative images of NP$_{miR199a-3p}$ and MMNP$_{miR199a-3p}$ examined with transmission electron microscopy (TEM). Samples were stained with uranyl acetate. Scale bar, 100 nm

We further analyzed the size and surface potential of $NP_{miR\text{-}199a\text{-}3p}$ and $MMNPmiR_{199a\text{-}3p}$. We found membrane-enveloped $MMNPmiR_{199a\text{-}3p}$ had bigger size than $NP_{miR\text{-}199a\text{-}3p}$ (Figure 1c) and these two kinds of NPs had opposite surface potentials (Figure 1d). The morphology of $NP_{miR\text{-}199a\text{-}3p}$ and $MMNPmiR_{199a\text{-}3p}$ was further analyzed by cryogenic transmission electron microscope (cryo-TEM) (Figure 1e). The membrane envelop was observed in $MMNPmiR_{199a\text{-}3p}$.

2.1.1 | $MMNP_{miR199a\text{-}3p}$ binds to inflammatory cytokines

Since the $MMNP_{miR199a\text{-}3p}$ was coated by the membrane of engineered macrophage, which had enhanced expression of IL-1βR, IL-6R, and TNF-αR, we characterized the expression of IL-1βR, IL-6R, and TNF-αR and potential cytokines binding ability of $MMNPmiR_{199a\text{-}3p}$. As shown in Figure 2a, we detected large amount of IL-1βR, IL-6R, and TNF-αR in membrane fraction of macrophage as well as in $MMNPmiR_{199a\text{-}3p}$. In contrast, IL-1βR, IL-6R, and TNF-αR were not detected in $NPmiR_{199a\text{-}3p}$. We continued to test the binding ability of $MMNPmiR_{199a\text{-}3p}$ to IL-1β, IL-6, and TNF-α. We incubated IL-1β, IL-6, and TNF-α with difference amounts of $MMNPmiR_{199a\text{-}3p}$ or $NPmiR_{199a\text{-}3p}$. After removal of NPs, the remaining cytokines in the supernatant were detected. As shown in Figure 2b, the level of remaining IL-1β in the supernatant of $MMNPmiR_{199a\text{-}3p}$ /IL-1β mixture decreased with increased concentration of $MMNPmiR_{199a\text{-}3p}$, indicating $MMNPmiR_{199a\text{-}3p}$ bound to IL-1β. In contrast, the level of remaining IL-1β in the supernatant of $NPmiR_{199a\text{-}3p}$/IL-1β mixture did not change with increased concentration of $NPmiR_{199a\text{-}3p}$, indicating $NPmiR_{199a\text{-}3p}$ did not bind to IL-1β. Similarly, we also found only $MMNPmiR_{199a\text{-}3p}$ bound to IL-6 (Figure 2c) and TNF-α (Figure 2d).

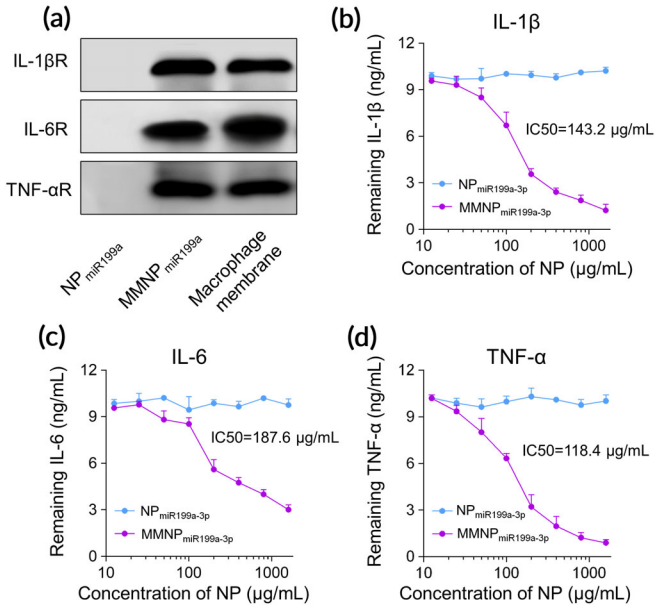

FIGURE 2 $MMNP_{miR199a\text{-}3p}$ can bind to inflammatory cytokines. (a) Characteristic protein bands of $NP_{miR199a\text{-}3p}$ and $MMNP_{miR199a\text{-}3p}$ examined by western blotting, macrophage membrane lysate was set as positive control. Binding capacity of $MMNP_{miR199a\text{-}3p}$ with IL-1β (b), IL-6 (c), and TNF-α (d). Recombinant mouse IL-1β, IL-6, and TNF-α (10 ng/ml) was mixed with $NP_{miR199a\text{-}3p}$ and $MMNP_{miR199a\text{-}3p}$ at final concentrations ranging from 0 to 1.6 mg/ml. The mixtures were incubated for 2 h at 37°C and nanoparticles were removed by centrifugation. The remaining proteins were examined by ELISA

2.2 | $NP_{miR199a\text{-}3p}$ and $MMNP_{miR199a\text{-}3p}$ promoted murine cardiovascular cells proliferation under hypoxic condition

As miR-199a-3p is a hypoxia-related miRNA and has been shown to induce cardiomyocyte proliferation,[21-23] we continued to evaluate the potential effects of $NP_{miR199a\text{-}3p}$ and $MMNP_{miR199a\text{-}3p}$ on proliferation of murine cardiovascular cells. First, we tested the uptake of Cy labeled miR-199a-3p by HL-1 cells. HL-1 cells incubated with $NP_{Cy5\text{-}miR199a\text{-}3p}$ and $MMNP_{Cy5\text{-}miR199a\text{-}3p}$ had significantly increased Cy5 signal (Figure 3a,b). In contrast, HL-1 cells incubated with free Cy5 labeled miR-199a-3p had no Cy5 signal. These results indicated that HL-1 cells uptook $NP_{Cy5\text{-}miR199a\text{-}3p}$ and $MMNP_{Cy5\text{-}miR199a\text{-}3p}$ but did not uptake free Cy5-miR-199a-3p. Interestingly, we detected similar Cy5 intensity between HL-1 cells mixed with $NP_{Cy5\text{-}miR199a\text{-}3p}$ and HL-1 cells mixed with $MMNP_{Cy5\text{-}miR199a\text{-}3p}$, suggesting HL-1 cells had similar efficacy of uptaking these two kinds of NPs. We also compared the miRNA delivery efficiency between NPs and Lipofecatime 2000 and found all delivery approach can efficiently deliver the miRNA into cells and Lipofectamine 2000 had slightly higher miRNA delivery efficacy compared with NP and MMNP. In addition, $NP_{Cy5\text{-}miR199a\text{-}3p}$ and $MMNP_{Cy5\text{-}miR199a\text{-}3p}$ treatment resulted in similar level of apoptosis when compared to Lipofectamine 2000, indicating NPs did not cause obvious cell toxicity (Figure S1). Correspondingly, confocal analysis confirmed the uptake of $NP_{Cy5\text{-}miR199a\text{-}3p}$ and $MMNP_{Cy5\text{-}miR199a\text{-}3p}$ Cy5 signal by HL-1 cells (Figure 3c). To test the effects of NPs on apoptosis under hypoxia condition, we pretreated HL-1 cells with NPs for 24 h and then cultured the cells under hypoxic condition. As shown in Figure 3d, we detected increased PI/Annexin V double positive cells in HL-1 cells cultured under hypoxia condition, indicating hypoxia induced apoptosis in HL-1 cells. Free miR199a-3a, which was not up-taken by HL-1 cells, did not affect the percentage of PI/Annexin V double positive cells, indicating free miR199a-3a did not affect hypoxia-induced apoptosis in HL-1 cells. In contrast, $NP_{miR199a\text{-}3p}$ and $MMNP_{miR199a\text{-}3p}$ significantly decreased the percentage of PI/Annexin V double positive cells, indicating miR199a-3p, which was up-taken by HL-1 suppressed hypoxia-induced apoptosis in HL-1 cells. As HL-1 cells had similar uptaking efficacy of $NP_{miR199a\text{-}3p}$ and $MMNP_{miR199a\text{-}3p}$, there was no significant difference of apoptotic cell percentage between HL-1 cells pretreated with $NP_{miR199a\text{-}3p}$ and those pretreated with $MMNP_{miR199a\text{-}3p}$ (Figure 3e). Correspondingly, we detected significantly increased cell viability in HL-1 pretreated with $NP_{miR199a\text{-}3p}$ and $MMNP_{miR199a\text{-}3p}$ when compared to HL-1 cells without treatment or treated with free miR199a-3p after hypoxia culture (Figure 3f). Hypoxia suppressed the expression of cell cycle-related genes, including Cell Division Cycle 6 (CDC6) (Figure 3g), Cyclin E1 (CCNE1) (Figure 3h), Cyclin

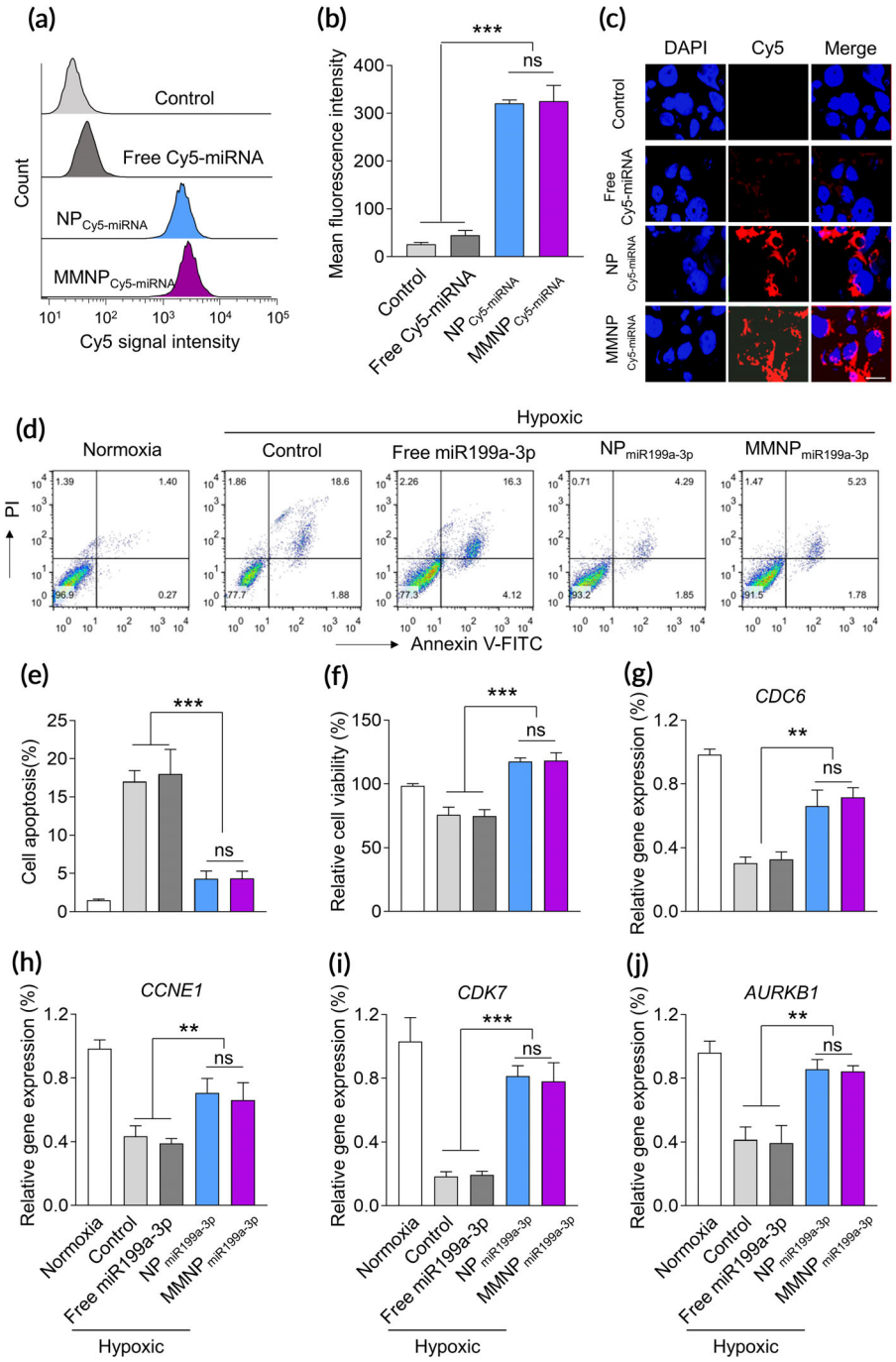

FIGURE 3 $NP_{miR199a-3p}$ and $MMNP_{miR199a-3p}$ promote the proliferation of murine cardiovascular cells under hypoxic condition. (a) Flow cytometric analysis of HL-1 cardiac muscle cell after 4 h incubation with free or nanoparticle encapsulated Cy5-labeled miRNA. The concentration of Cy5-miRNA was 100 nM. (b) Mean fluorescence intensity based on the flow cytometric analysis. Data represent means ± SD. ns, no significant difference. ***$p < .001$. (c) Confocal microscopic images show the cellular uptaken of $NP_{Cy5\text{-}miRNA}$ and $MMNP_{Cy5\text{-}miRNA}$. (d) Cell viability of HL-1 cells after treated with different formulations. To generate hypoxic culture condition, HL-1 cells culture was carried out in a hypoxic incubator containing 1% O_2 for 6 h at 37°C. Cells were treated with free miR199a-3p, $NP_{miR199a-3p}$, and $MMNP_{miR199a-3p}$ (100 nM) for 24 h before hypoxic culture. Cell apoptosis and proliferation were examined after culture in hypoxic condition for 24 h. (d) and (e) Cell apoptosis were detected by flow cytometry after stained with PI and Annexin V-FITC. (f) Cell viabilities were examined by MTT assay. The cell cycle related genes, including CDC6 (g), CCEN1 (h), CDK7 (i), and AURKB (j), were examined by real-time PCR. Cells were treated as the MTT assay. Data represent means ± SD. ns, no significant difference. **$p < .01$, ***$p < .001$

Dependent Kinase 7 (CDK7) (Figure 3i), and AURKB1 (Figure 3j). Free miR199a-3p did not affect the expression of these genes. In contrast, pretreatment of $NP_{miR199a-3p}$ and $MMNP_{miR199a-3p}$ significantly increased the mRNA level of these genes, indicating miR199a-3p ameliorated the expression of these genes in hypoxia condition.

2.3 | $MMNP_{miR199a-3p}$ suppressed inflammation in mice with acute MI

We continued to evaluate the effects of $MMNP_{miR199a-3p}$ on MI *in vivo*. After intravenously administration in mice, NPs containing Cy5-labeled miRNA can be detected in multiple organs, including the heart, suggesting NPs could display potential function in local area of heart (Figure S2). We administered free miR199a-3p, $NP_{miR199a-3p}$, $MMNP_{miRNA-sc}$ (MMNP containing scramble miRNA), and $MMNP_{miR199a-3p}$ to mice with MI (Figure 4a) and evaluated the inflammatory response. MI mice had significantly increased local level of IL-1β (Figure 4b), IL-6 (Figure 4c), and TNF-α (Figure 4d) in peri-infarct tissues when compared to sham mice. Administration of free miR199a-3p did not affect the cytokine level of IL-1β (Figure 4b), IL-6 (Figure 4c), and TNF-α (Figure 4d) in peri-infarct tissues. Administration of $NP_{miR199a-3p}$ slightly decreased the level of IL-1β, IL-6, and TNF-α in peri-infarct tissues, indicating the anti-inflammatory activity

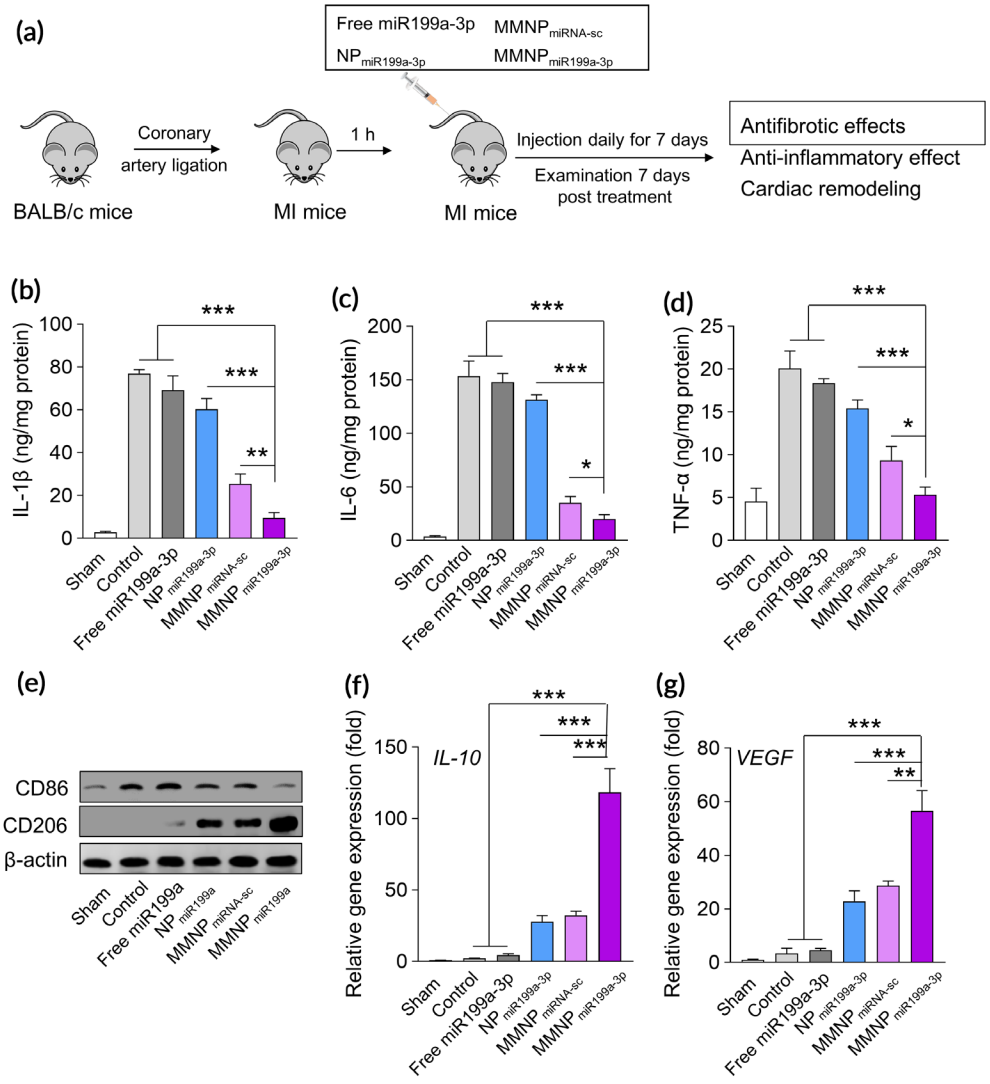

FIGURE 4 $MMNP_{miR199a-3p}$ treatment attenuates inflammation in vivo. (a) Schematic depicts the experiment protocol. The mice model of myocardial infarction (AMI) was established by ligating the proximal left coronary artery of male Balb/c mice for 30 minutes and then release. Mice were intravenously administrated with PBS (control group), free miR199a-3p, $NP_{miR199a-3p}$, $MMNP_{miRNA-sc,}$ and $MMNP_{miR199a-3p}$, the injection dosage of miR199a-3p and miR-199a-3p scramble mimic was 2.0 mg/kg, mice were treated daily for 7 days, and the antifibrotic effects, anti-inflammatory effect and cardiac remodeling were examined two week post last injection. The concentration of IL-1β (b), IL-6 (c), and TNF-α (d) in the peri-infarct zone were detected by ELISA. (e) The expressions of CD86 and CD206 in the peri-infarct zone two-week post treatment were examined by western blot. The expressions of M2 macrophages related genes, including IL-10 (f) and VEGF (g) were examined by real-time PCR. Data represent means ± SD. $n = 8$. $^{*}p < .05$, $^{**}p < .01$, $^{***}p < .001$

of miR199a-3p. Administration of $MMNP_{miRNA-sc}$ also decreased the level of IL-1β, IL-6, and TNF-α, indicating the membrane associated IL-1βR, IL-6R, and TNF-αR functioned to blocked the IL-1β, IL-6, and TNF-α. We detected the significantly decreased level of IL-1β, IL-6, and TNF-α in peri-infarct tissues of MI mice treated with $MMNP_{miR199a-3p}$, indicating $MMNP_{miR199a-3p}$ had the best inhibitory effect on inflammation in MI mice. We further tested the expression of M1 macrophage marker CD86 and M2 marker CD206 in peri-infarct tissues. As shown in Figure 4e, we detected increased CD86 in peri-infarct tissues of MI mice. Administration of free miR199a-3p did not affect CD86 expression. In contrast, administration of $NP_{miR199a-3p}$, $MMNP_{miRNA-sc,}$ and $MMNP_{miR199a-3p}$ decreased the CD86 expression in peri-infarct tissues, indicating these treatments suppressed the inflammation. Correspondingly, $NP_{miR199a-3p}$, $MMNP_{miRNA-sc,}$ and $MMNP_{miR199a-3p}$ promoted the expression of CD206. Mice administrated with $MMNP_{miR199a-3p}$ had the lowest level of CD86 and the highest level of CD206 in peri-infarct tissues, indicating $MMNP_{miR199a-3p}$ had the best anti-inflammatory activities. Similarly, we detected the significantly increased mRNA level of IL-10 (Figure 4f) and vascular endothelial growth factor (VEGF) (Figure 4g), two proteins produced by M2 macrophages, in the peri-infarct tissues.

2.4 | $MMNP_{miR199a-3p}$ suppressed the expression of fibrosis-related proteins

To evaluate the effects of $MMNP_{miR199a-3p}$ on fibrosis in MI mice, we detected the expression level of fibrosis related genes, including TGFβ, ACTA2, MMP2, MMP9, TIMP1, and TIMP2.[24] MI mice had elevated mRNA level of TGFβ (Figure 5a), ACTA2 (Figure 5b), MMP2 (Figure 5c), MMP9 (Figure 5d), TIMP1 (Figure 5e), and TIMP2 (Figure 5f). Administration of free miR199a-3p slightly decreased the mRNA level of TGFβ, ACTA2, MMP2, MMP9, TIMP1, and TIMP2. $NP_{miR199a-3p}$ and $MMNP_{miRNA-sc}$ treatment also decreased the mRNA level to a lower level when compared to free miR199a-3p. $MMNP_{miR199a-3p}$ treatment dramatically down-regulated the mRNA level of TGFβ, ACTA2, MMP2, MMP9, TIMP1, and TIMP2 and the mRNA level of these genes was significantly lower than other treatment.

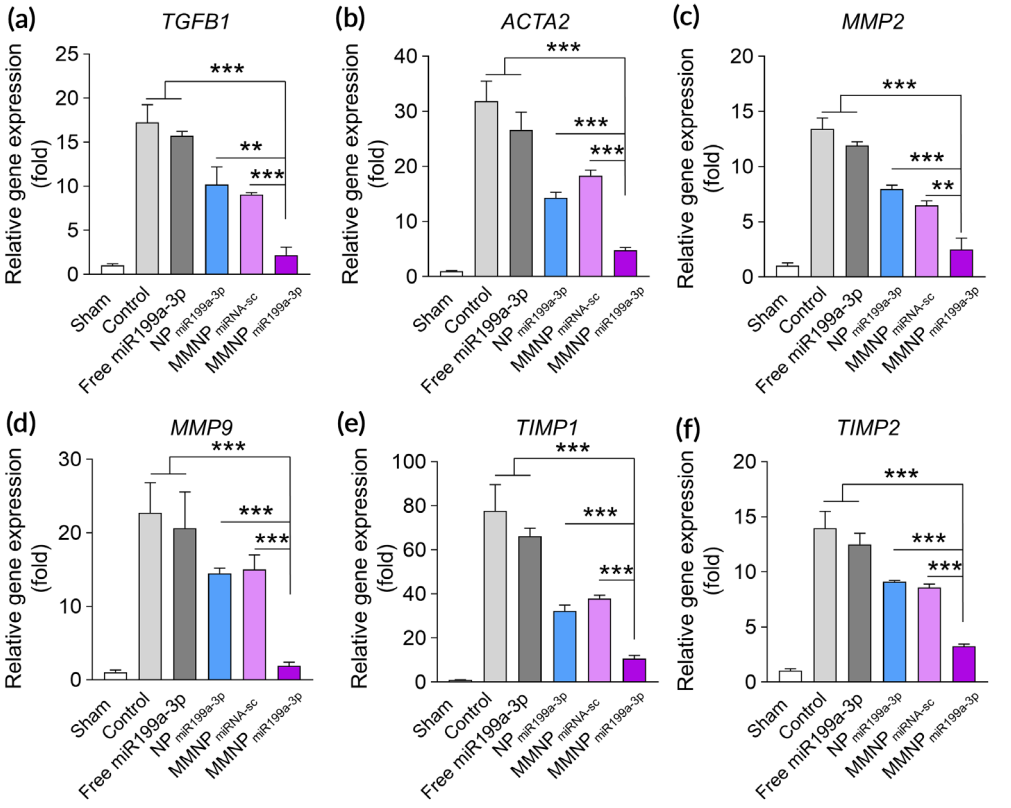

FIGURE 5 Administration of $MMNP_{miR199a\text{-}3p}$ inhibits expression of cardiac fibrosis markers. Relative mRNA expression levels of cardiac myofibroblast-related genes, including TGFβ (a), ACTA2 (b), MMP2 (c), MMP9 (d), TIMP1 (e), and TIMP2 (f) in the peri-infarct zone two week after treatment, as evaluated by real-time PCR. Data represent means ± SD. $n = 8$. $^{**}p < .01$, $^{***}p < .001$

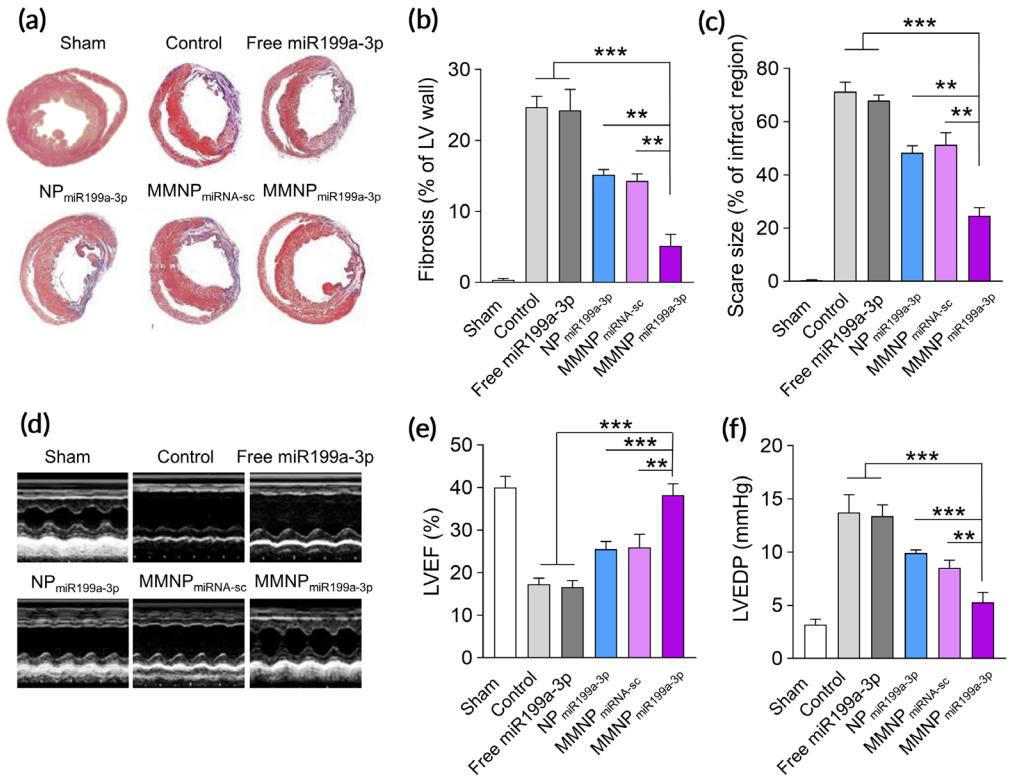

FIGURE 6 Administration of $MMNP_{miR199a}$ improves left ventricular remodeling and promote cardiac function recovery. (a) Representative Masson's trichrome–stained infarcted hearts two weeks after treatment (blue, scar tissue; red, viable myocardium). The fibrosis area (b) and scar size (c) of the left ventricular (LV) wall one weeks after treatment. (d) Representative M-mode images 2 weeks after treatment. (e) Left ventricular ejection fraction (LVEF). (f) Hemodynamic analyses of LV end diastolic pressure (LVEDP). Data represent means ± SD. $n = 8$. $^{**}p < .01$, $^{***}p < .001$

2.5 | Administration of $MMNP_{miR199a}$ protected against cardiac injury in MI mice

We continued to evaluate the effects of $MMNP_{miR199a}$ on cardiac injury and function in MI mice. We used Masson's trichrome staining to stain the transverse and coronal plane and detected obvious myocardial fibrotic area in control MI mice (Figure 6a). MI mice treated with free miR199a-3p has similar myocardial fibrotic area to control mice. In contrast, MI mice treated with $NP_{miR199a\text{-}3p}$, $MMNP_{miRNA\text{-}sc}$, and $MMNP_{miR199a\text{-}3p}$ had obvious decreased myocardial fibrotic area

(Figure 6a). After quantitation, we found $MMNP_{miR199a-3p}$ significantly decreased both fibrosis (Figure 6b) and scare size (Figure 6c) when compared to no treatment, $NP_{miR199a-3p}$ or $MMNP_{miRNA-sc}$. In addition, MI mice had dramatically decreased LV ejection fraction while $MMNP_{miR199a-3p}$ treatment increased LV ejection fraction significantly more than $NP_{miR199a-3p}$ or $MMNP_{miRNA-sc}$ treatment (Figure 6d,e). Relatively, $MMNP_{miR199a-3p}$ treatment significantly decreased the Left ventricular end diastolic pressure (Figure 6f).

3 | DISCUSSION

In the present study, we investigated the potential protective effects of macrophage membrane coated NPs containing miR199a-3p ($MMNP_{miR199a-3p}$) on MI. The membranes were extracted from engineered macrophages overexpressing receptors of TNF-α, IL-1, and IL-6. We demonstrated that the $MMNP_{miR199a-3p}$ absorbed inflammatory cytokines TNF-α, IL-1, and IL-6, and can be efficiently up-taken by cardiovascular cells. The up-taken $MMNP_{miR199a-3p}$ prevented hypoxia-induced cell apoptosis and promoted the proliferation of cardiovascular cells. The $MMNP_{miR199a-3p}$ inhibited the inflammatory response by decreasing inflammatory cytokine level in MI mice and converted a M2 phenotype environment in peri-infarct zone. In addition, $MMNP_{miR199a-3p}$ prevented fibrosis, improved left ventricular remodeling, and promoted cardiac function. Therefore, these results suggested $MMNP_{miR199a-3p}$ could be utilized as a potential effective approach to treat MI.

Myocardial infarction is the leading cause of death. Cell apoptosis and cardiac fibrosis are two important events occur after MI. Apoptosis plays an significant role in myocardial loss after MI and is involved in the process of subsequent left ventricular remodeling and development of heart failure.[3] In MI, dominant apoptosis is present and correlated with left ventricular remodeling.[25] Using animal model, Bialik et al described that MI resulted in apoptosis, which only emerged in hypoxic regions during acute infarction. The hypoxia-induced apoptosis was independent of p53.[26] Inhibition of apoptosis has been shown to protect left ventricular function and attenuate remodeling in MI rats.[27] Therefore, targeting apoptosis could be a useful approach to treat MI. miRNAs are small, non-coding RNAs, which can silence gene by inhibiting mRNA translation.[28] Increasing evidences have shown that miRNA is involved in the pathogenesis of MI.[29] For example, he and colleagues reported that inhibition of miR-124 inhibited cardiomyocytes apoptosis and protected against MI.[30] Overexpressing miR-325-3p attenuated the cardiac tissue injury and decreased the infarct size.[31] MiR199a-3p has been described to regulate the cardiac cell proliferation and inducing cardiac regeneration after MI, either when expressed by adeno-associated virus (AAV) vector[32] or directly intra-cardiac injection.[13] These results suggested miR199a-3p was a potential candidate for MI treatment. In the present study, we utilized NPs containing miR199a-3p as the approach for treatment. We demonstrated that NPs containing miR199a-3p ($NP_{miR199a-3p}$ and MM $NP_{miR199a-3p}$) prevented hypoxia-induced apoptosis of cardiovascular cells, promoted the expression of cell cycle related proteins, and induced cell proliferation. Interestingly, the free miR199a-3p, which was directly added to the cell culture had no effect on these parameters. We found that the cardiovascular cells HL-1 cells only up-took NPs containing Cy5-labeled miR199a-3p but not the free Cy5-labled miR199a-3p. These results strongly suggested that the correct and efficient delivery approach is one key factor in designing disease treatment. The CLAN NPs is an efficient delivery system to deliver the miRNA into target cells and enable the active function of miRNA in cells.

MI also induces inflammatory response and cytokine production. Robust production of pro-inflammatory cytokines, including TNF-α, IL-1β, and IL-6 has been detected after MI induction in rodents.[33] The excessive inflammatory responses promote fibrosis and results in pathological remodeling and the progression of myocardial disease. Therefore, it has been suggested that inflammation could be an important target for disease preventing.[34] Li and colleagues produced microparticles with anti-IL-1β antibodies and they found that these microparticles neutralized IL-1β after MI, prevented cardiac remodeling, and induced cardiac repair.[8] In present study, we utilized the membrane from macrophages overexpressing the receptors of TNF-α, IL-1β, and IL-6 and coated to the $NP_{miR199a-3p}$. We found that the macrophage membrane coated $NP_{miR199a-3p}$ ($MMNP_{miR199a-3p}$) can bind to and absorb TNF-α, IL-1β, and IL-6 while $NP_{miR199a-3p}$ cannot. In MI mice, the $MMNP_{miR199a-3p}$ had significantly enhanced anti-inflammatory activities compared to $NP_{miR199a-3p}$, suggesting the membranes containing TNF-αR, IL-1βR, and IL-6R contribute to the anti-inflammatory activities of $MMNP_{miR199a-3p}$. Our findings are similar to previous study, which described that the neutrophil membrane-coated NPs neutralized pro-inflammatory cytokines and protected against joint damage.[19] In the present study, delivery of $NP_{miR199a-3p}$ also resulted in decreased inflammation in peri-infarct tissues, indicating miR199a-3p itself had the anti-inflammatory activities. Previous study by Bardin et al described that miR-199a-3p negatively regulated IκB Kinase β (IKKβ) expression and inhibited the nuclear factor kappa-light-chain-enhancer of activated B cells (NF-κB) signaling pathway.[35] This result supported our finding that miR199a-3p itself suppressed inflammation. However, the underlying mechanism of how miR199a-3p inhibits inflammation need to be further investigated. It should be interesting to detect the NF-κB activation in MI heart after administration of $NP_{miR199a-3p}$.

Several questions of current study need to be further addressed. We found the differences of anti-inflammatory activity between $NP_{miR199a-3p}$ and $MMNP_{miR199a-3p}$. The cytokines absorption ability of $MMNP_{miR199a-3p}$ should contribute to the differences. It has been described that the cell membrane coated NPs is with the biological properties of the source cell from which their membrane is derived, and have prolonged circulation and disease-relevant targeting.[36] It is well-known that the macrophages accumulate into heart after MI and play significantly role.[37] It is possible that the $MMNP_{miR199a-3p}$ should better target to heart tissue when compared to $NP_{miR199a-3p}$ in MI mice while direct evidence and careful comparison are needed. In addition, to maximize the effects of NPs in MI heart, it is desired to enhance the biodistribution of NPs in MI heart. The factors involved in NPs distribution should be evaluated.

4 | MATERIALS AND METHODS

4.1 | Nanoparticle preparation and characterization

MiR199a-3p, Cy5 labeled miR199a-3p and control miRNA were obtained from RiboBio Co. (Guangzhou, China). CLAN containing miR199a-3p was prepared using double emulsion method as described previously.[38] Briefly, 25 mg $mPEG_{5K}$-b-$PLGA_{11K}$, 2 mg BHEM-Chol in chloroform, and 200 mg miR199a-3p (Ribobio, Guangzhou, China) in DNase/RNase free water were emulsified. Then another emulsion was performed. After this, the chloroform was evaporated. The NPs containing miR-199a-3p was termed as $NP_{miR199a\text{-}3p}$.

Macrophage membrane enveloped NPs were prepared as previously described.[39] RAW 264.7 cells were transfected plasmids encoding IL-1βR, IL-6R, and TNF-αR (Origene, Beijing China) using Lipofectamine LTX Reagent (Thermo Fisher, Waltham, MA) following manufacture's protocol. 48 h post transfection, cells were harvested and homogenized in hypotonic lysis buffer (20 mM Tris–HCl, 10 mM KCl, 2 mM $MgCl_2$) containing protease inhibitor. After centrifuge at 3200 g for 5 min, the supernatant was saved and the pellet was re-homogenized again. The supernatant was pooled and centrifuged at 20,000 g for 30 min at 4°C. The supernatant was ultra-centrifuged at 80,000 g for 2 h and the pellets containing the plasma membrane were collected. Finally, the pellets were extruded through a 400-nm polycarbonate porous membrane to get the membrane materials.

To make membrane enveloped NPs, the NPs were suspended in phosphate-buffered saline (PBS) and mixed with prepared macrophage membranes. The mixture was then extruded. After centrifuge, the newly prepared MMNPs were suspended in PBS and stored at 4°C.

The diameters and zeta potentials of NPs were measured using Zetasizer Nano ZS90 analyzer (Malvern Panalytical Ltd, Malvern, United Kingdom). The FEI Artica Cryogenic-Biological transmission electron microscopy (TEM) was used to detect the morphology of NPs.

4.2 | Quantification of cytokine binding

To test the cytokine binding ability, 10 ng/ml mouse IL-1β, IL-6, or TNF-α was mixed with 0 to 1.6 mg/ml $NP_{miR199a\text{-}3p}$ or $MMNP_{miR199a\text{-}3p}$. The mixtures were incubated at 37°C for 2 h. Then the NPs were removed by centrifugation at 13,000 rmp for 10 min. Cytokine concentration in the supernatant was measured using commercial mouse IL-1β, IL-6, or TNF-α enzyme-linked immunosorbent assay (ELISA) kit (Abcam, Beijing, China).

4.3 | Cell culture

Cardiac myocyte cell line HL-1 cells were purchased from Sigma (St. Louis, MO) and cultured in Claycomb medium supplemented with 10% heat-inactivated fetal bovine serum (FBS), 2 mM L-glutamine, 100 U/ml Penicillin, 100 μg/ml Streptomycin, and 100 μM norepinephrine. Cells were maintained under an atmosphere of 5% CO_2 at 37°C. For hypoxic condition, HL-1 cells were cultured in a hypoxic incubator containing 1% O_2 for 6 h at 37°C.

4.4 | MTT assay

3-(4,5-Dimethylthiazol-2-yl)-2,5-diphenyltetrazolium bromide (MTT, Sigma) assay was used to detect HL-1 cell proliferation. Briefly, HL-1 cells were seeded in 96-well plate. After treatment, cells were treated with 100 nM free miR199a-3p, or $NP_{miR199a\text{-}3p}$ or $MMNP_{miR199a\text{-}3p}$ containing 100 nM miR199a-3p for 24 h and then incubated in a hypoxic incubator for 6 h. After culture for another 24 h at normal condition, 20 μl MTT reagents (5 mg/ml, Abcam, Beijing, China) was added to each well and incubated for 1 h at 37°C. The remaining crystals were dissolved in dimethyl sulfoxide. The absorbance at 492 nm was measured.

4.5 | Apoptosis analysis

The FITC Annexin V Apoptosis Detection Kit with PI (Biolegend, San Diego, CA) was used to detect apoptosis according to manufacturer's protocols. After staining, cells were analyzed by flow cytometry using FACS Calibur (BD bioscience, San Jose, CA) and FlowJo software.

4.6 | Reverse transcription polymerase chain reaction (RT-PCR)

Total RNA from HL-1 cells or tissues was extracted using RNeasy Mini Kit (Qiagen, Germantown, MD). Then the cDNA was synthesized by reverse transcription using the PrimeScript™ RT Reagent Kit (Takara, Beijing, China). Real time quantitative PCR reactions were set up with TB Green® Advantage® qPCR Premix (Takara, China) and performed using the QuantStudio 3 Real-time PCR System (Applied biosystems). Primers used for real time PCR included: *cdc6* forward: 5′-TCTTGACACTTCCAGTCGAAGGA-3′, reverse: 5′-TAGAGTCGCTG TGAGGCCACGACCACTG-3′. *Cyclin E1* forward: 5′-GCCAGCCTTG GGACAATAATG-3′, reverse: 5′-AGTTTGGGTAAACCCGGTCAT-3′. *cdk7* forward: 5′-AGGATGTATGGTGTAGGTGTGGA-3′, reverse: 5′-AAGATGTGATGCAAAGGTATTCC-3′. *AURKB* forward: 5′- TCCCTGT TCGCATTCAACCT-3′, reverse: 5′- GTCCCACTGCTATTCTCCAT CAC-3′. *IL-10* forward: 5′-AAGGCAGTGGAGCAGGTGAA-3′, reverse: 5′-CCAGCAGACTCAATACACAC-3′. VEGF forward: 5′- GGAGAT CCTTCGAG GAGCACTT-3′, reverse: 5′- GGCGATTTAGCAGCAGAT ATAAGAA-3′. *TGFβ* forward: 5′-CCTGTCCAAACTAAGGC-3′, reverse: 5′-GGTTTTCTCATAGATGGCG-3′. ACTA2 forward: 5′-ACTGGGA CGACATGGAAAAG-3′, reverse: 5′-GTTCAGTGGTGCCTCTGTCA-3′. *MMP-2* forward: 5′-AAGGATGGACTCCTGGCACATGCCTTT-3′, reverse:5′- ACCTGTGG GCTTGTCACGTGGTGT-3′. *MMP-9* forward: 5′-AAGGACGGCCTTCTGGCACACGCCT TT-3′, reverse: 5′-GTGGTATA GTGGGACACATAGTGG′3′. *TIMP1* forward: 5′-CCCAGA AATCAA CGAGA-3′, reverse: 5′-TGGGACTTGTGGGCATA-3′. *TIMP2* forward: 5′- AAGCGGTCAGTGAGAAGGAGTGG-3′, reverse 5′-CCTTGGAG

GCTTTTTTGCAGTTG-3′. *Glyceraldehyde-3-phosphate dehydrogenase (GAPDH)* forward 5′-AGAAGGCTGGGGCTCATTTC-3′, reverse 5′-AGGGGCCATCC ACAGT CTTC-3′. The relative amount of target gene mRNA was normalized to *GAPDH* mRNA. Expression levels of specific genes were normalized against the Sham group.

4.7 | ELISA

Tissues were homogenized in tissue extraction buffer (Abcam, Beijing, China) and homogenates were centrifuged for 20 min at 13,000 rpm at 4°C. The levels of IL-1β, IL-6, and TNF-α were measured using commercial ELISA kit from Abcam (Beijing, China) following manufacturer's protocols.

4.8 | Western blot

The western blot was performed as described previously.[40] Briefly, NPs, MMNPs, macrophage membrane extraction, or total protein extracted from heart tissues were subjected to sodium dodecyl sulfate–polyacrylamide gel electrophoresis and then were transferred to polyvinylidene fluoride membranes. The membranes were blocked with 5% non-fat milk for overnight at 4°C. Next day, primary antibodies were added to the membrane and incubated at room temperature for 2 h. After wash, corresponding horse radish peroxidase-conjugated secondary antibodies were incubated for 1 h at room temperature. Immuno-reactive bands were visualized using ECL substrate kit (Abcam, China). Antibodies used in present study include: anti-IL-1R (Abcam, Beijing, China), anti-IL-6R (Abcam, China), anti-tumor necrosis factor receptor 1 (TNFRI) (Abcam, China), anti-CD86 (Abcam, China), and anti-CD206 (Abcam, China).

4.9 | Immunofluorescence assay

HL-1 cardiac muscle cells were incubated with free or nanoparticle encapsulated Cy5-labeled miRNA for 4 h. Then the cells were washed with PBS and fixed with 4% paraformaldehyde. The DNA was stained with 4′,6-diamidino-2-phenylindole (DAPI) (Thermo Fisher) at room temperature for 5 min. After wash, cells were analyzed by confocal microscopy.

4.10 | Mice treatment

MI was induced in Balb/c mice by coronary artery ligation as described previously.[41] 1 h post coronary artery ligation, 2.0 mg/kg free miRNAs or NPs were injected by tail vein every day for consecutive 7 days. After treatment, tissues were harvested for analysis. The study was approved by the ethics commitment of Tangdu Hospital, Air force Military Medical University.

4.11 | Masson staining

The fibrosis of heart was determined using Masson Trichrome Stain kit (Sigma, St. Louis, MO) following manufacturer's protocols. The collagen fibers were stained as blue and the viable myocardium was stained as red. The area of fibrosis and the scare size was quantitated using ImageJ software.

4.12 | Echocardiography and hemodynamic study

Mice were anesthetized by isoflurane and then M-mode images were obtained by using Visualsonics Vevo 770 echocardiography machine (Visualsonics Inc., Toronto, Canada) as described previously.[42] Hearts areas between two papillary muscles were viewed. LV internal dimensions (LVID) at diastole (LVIDd) and systole (LVIDs) were measured. The LV ejection fraction (EF) was calculated by the software with the machine. The cardiac hemodynamic function was evaluated using a Millar tip-pressure catheter as described previously.[42] LV end-diastolic pressure (LVEDP) was measured by catheter advancement into the LV cavity. Data were analyzed using the PowerLab System.

4.13 | Statistical analysis

All data are shown as means ± standard deviations (SD). Statistical analysis was performed by one-way ANOVA followed with a Tukey's post hoc test. $p < .05$ was considered statistically significant.

CONFLICT OF INTEREST

No conflicts of interest, financial, or otherwise, are declared by the authors.

AUTHOR CONTRIBUTIONS

Yugang Xue: Data curation; investigation; software; supervision; validation. **Guangwei Zeng:** Data curation; formal analysis; resources. **Jin Cheng:** Data curation; formal analysis; funding acquisition. **Mingming Zhang:** Supervision; validation; writing-original draft; writing-review and editing. **Jianqiang Hu:** Methodology; validation; visualization. **Yan Li:** Funding acquisition; resources; supervision; writing-original draft; writing-review and editing.

PEER REVIEW

The peer review history for this article is available at https://publons.com/publon/10.1002/btm2.10197.

DATA AVAILABILITY STATEMENT

Data could be obtained upon reasonable request to the corresponding author.

ORCID

Guangwei Zeng https://orcid.org/0000-0001-7025-1209
Yan Li https://orcid.org/0000-0003-0096-0813

REFERENCES

1. Thygesen K, Alpert JS, Jaffe AS, et al. Third universal definition of myocardial infarction. *Nat Rev Cardiol*. 2012;9(11):620-633.
2. Chiang MH, Liang CJ, Lin LC, et al. miR-26a attenuates cardiac apoptosis and fibrosis by targeting ataxia-telangiectasia mutated in myocardial infarction. *J Cell Physiol*. 2020;235(9):6085-6102.

3. Teringova E, Tousek P. Apoptosis in ischemic heart disease. *J Transl Med*. 2017;15(1):87.
4. Chang H, Li C, Wang Q, et al. QSKL protects against myocardial apoptosis on heart failure via PI3K/Akt-p53 signaling pathway. *Sci Rep*. 2017;7(1):16986.
5. Talman V, Ruskoaho H. Cardiac fibrosis in myocardial infarction-from repair and remodeling to regeneration. *Cell Tissue Res*. 2016;365(3):563-581.
6. Liu J, Wang H, Li J. Inflammation and inflammatory cells in myocardial infarction and reperfusion injury: a double-edged sword. *Clin Med Insights Cardiol*. 2016;10:79-84.
7. Nian M, Lee P, Khaper N, Liu P. Inflammatory cytokines and postmyocardial infarction remodeling. *Circ Res*. 2004;94(12):1543-1553.
8. Li Z, Hu S, Huang K, Su T, Cores J, Cheng K. Targeted anti-IL-1beta platelet microparticles for cardiac detoxing and repair. *Sci Adv*. 2020;6(6):eaay0589.
9. Buckley LF, Abbate A. Interleukin-1 blockade in cardiovascular diseases: a clinical update. *Eur Heart J*. 2018;39(22):2063-2069.
10. Holte E, Kleveland O, Ueland T, et al. Effect of interleukin-6 inhibition on coronary microvascular and endothelial function in myocardial infarction. *Heart*. 2017;103(19):1521-1527.
11. Berry MF, Woo YJ, Pirolli TJ, et al. Administration of a tumor necrosis factor inhibitor at the time of myocardial infarction attenuates subsequent ventricular remodeling. *J Heart Lung Transplant*. 2004;23(9):1061-1068.
12. Kumarswamy R, Thum T. Non-coding RNAs in cardiac remodeling and heart failure. *Circ Res*. 2013;113(6):676-689.
13. Lesizza P, Prosdocimo G, Martinelli V, Sinagra G, Zacchigna S, Giacca M. Single-dose intracardiac injection of pro-regenerative microRNAs improves cardiac function after myocardial infarction. *Circ Res*. 2017;120(8):1298-1304.
14. Yang H, Qin X, Wang H, et al. An in vivo miRNA delivery system for restoring infarcted myocardium. *ACS Nano*. 2019;13(9):9880-9894.
15. Bejerano T, Etzion S, Elyagon S, Etzion Y, Cohen S. Nanoparticle delivery of miRNA-21 mimic to cardiac macrophages improves myocardial remodeling after myocardial infarction. *Nano Lett*. 2018;18(9):5885-5891.
16. Hu CM, Fang RH, Wang KC, et al. Nanoparticle biointerfacing by platelet membrane cloaking. *Nature*. 2015;526(7571):118-121.
17. LaGrow AL, Coburn PS, Miller FC, et al. A novel biomimetic nanosponge protects the retina from the *Enterococcus faecalis* cytolysin. *mSphere*. 2017;2(6):e00335-17.
18. Hu CM, Fang RH, Copp J, Luk BT, Zhang L. A biomimetic nanosponge that absorbs pore-forming toxins. *Nat Nanotechnol*. 2013;8(5):336-340.
19. Zhang Q, Dehaini D, Zhang Y, et al. Neutrophil membrane-coated nanoparticles inhibit synovial inflammation and alleviate joint damage in inflammatory arthritis. *Nat Nanotechnol*. 2018;13(12):1182-1190.
20. Torrini C, Cubero RJ, Dirkx E, et al. Common regulatory pathways mediate activity of microRNAs inducing cardiomyocyte proliferation. *Cell Rep*. 2019;27(9):2759-2771 e2755.
21. Kinose Y, Sawada K, Nakamura K, et al. The hypoxia-related microRNA miR-199a-3p displays tumor suppressor functions in ovarian carcinoma. *Oncotarget*. 2015;6(13):11342-11356.
22. Baker AH, van Rooij E. miRNA overexpression induces cardiomyocyte proliferation in vivo. *Mol Ther*. 2013;21(3):497-498.
23. Shatseva T, Lee DY, Deng Z, Yang BB. MicroRNA miR-199a-3p regulates cell proliferation and survival by targeting caveolin-2. *J Cell Sci* 2011;124(Pt 16):2826–2836.
24. Liguori TTA, Liguori GR, Moreira LFP, Harmsen MC. Fibroblast growth factor-2, but not the adipose tissue-derived stromal cells secretome, inhibits TGF-beta1-induced differentiation of human cardiac fibroblasts into myofibroblasts. *Sci Rep*. 2018;8(1):16633.
25. Abbate A, Biondi-Zoccai GG, Bussani R, et al. Increased myocardial apoptosis in patients with unfavorable left ventricular remodeling and early symptomatic post-infarction heart failure. *J Am Coll Cardiol*. 2003;41(5):753-760.
26. Bialik S, Geenen DL, Sasson IE, et al. Myocyte apoptosis during acute myocardial infarction in the mouse localizes to hypoxic regions but occurs independently of p53. *J Clin Invest*. 1997;100(6):1363-1372.
27. Chandrashekhar Y, Sen S, Anway R, Shuros A, Anand I. Long-term caspase inhibition ameliorates apoptosis, reduces myocardial troponin-I cleavage, protects left ventricular function, and attenuates remodeling in rats with myocardial infarction. *J Am Coll Cardiol*. 2004;43(2):295-301.
28. O'Brien J, Hayder H, Zayed Y, Peng C. Overview of MicroRNA biogenesis, mechanisms of actions, and circulation. *Front Endocrinol (Lausanne)*. 2018;9:402.
29. Chen Z, Li C, Lin K, Zhang Q, Chen Y, Rao L. MicroRNAs in acute myocardial infarction: evident value as novel biomarkers? *Anatol J Cardiol*. 2018;19(2):140-147.
30. He F, Liu H, Guo J, et al. Inhibition of microRNA-124 reduces cardiomyocyte apoptosis following myocardial infarction via targeting STAT3. *Cell Physiol Biochem*. 2018;51(1):186-200.
31. Zhang DY, Wang BJ, Ma M, Yu K, Zhang Q, Zhang XW. MicroRNA-325-3p protects the heart after myocardial infarction by inhibiting RIPK3 and programmed necrosis in mice. *BMC Mol Biol*. 2019;20(1):17.
32. Eulalio A, Mano M, Dal Ferro M, et al. Functional screening identifies miRNAs inducing cardiac regeneration. *Nature*. 2012;492(7429):376-381.
33. Deten A, Volz HC, Briest W, Zimmer HG. Cardiac cytokine expression is upregulated in the acute phase after myocardial infarction. Experimental studies in rats. *Cardiovasc Res*. 2002;55(2):329-340.
34. Anzai T. Inflammatory mechanisms of cardiovascular remodeling. *Circ J*. 2018;82(3):629-635.
35. Bardin P, Marchal-Duval E, Sonneville F, et al. Small RNA and transcriptome sequencing reveal the role of miR-199a-3p in inflammatory processes in cystic fibrosis airways. *J Pathol*. 2018;245(4):410-420.
36. Yan H, Shao D, Lao YH, Li M, Hu H, Leong KW. Engineering cell membrane-based nanotherapeutics to target inflammation. *Adv Sci (Weinh)*. 2019;6(15):1900605.
37. Peet C, Ivetic A, Bromage DI, Shah AM. Cardiac monocytes and macrophages after myocardial infarction. *Cardiovasc Res*. 2020;116(6):1101-1112.
38. Luo YL, Xu CF, Li HJ, et al. Macrophage-specific in vivo gene editing using cationic lipid-assisted polymeric nanoparticles. *ACS Nano*. 2018;12(2):994-1005.
39. Rao LHZ, Meng Q-F, Zhou Z, et al. Effective cancer targeting and imaging using macrophage membrane-camouflaged upconversion nanoparticles. *J Biomed Mater Res*. 2017;105(2):521-530.
40. Jiang Y, Wang X, Yang W, Gui S. Procyanidin B2 suppresses lipopolysaccharides-induced inflammation and apoptosis in human type II alveolar epithelial cells and lung fibroblasts. *J Interferon Cytokine Res*. 2020;40(1):54-63.
41. Gao E, Lei YH, Shang X, et al. A novel and efficient model of coronary artery ligation and myocardial infarction in the mouse. *Circ Res*. 2010;107(12):1445-1453.
42. Yan W, Guo Y, Tao L, et al. C1q/tumor necrosis factor-related protein-9 regulates the fate of implanted mesenchymal stem cells and mobilizes their protective effects against ischemic heart injury via multiple novel signaling pathways. *Circulation*. 2017;136(22):2162-2177.

SUPPORTING INFORMATION

Additional supporting information may be found online in the Supporting Information section at the end of this article.

How to cite this article: Xue Y, Zeng G, Cheng J, Hu J, Zhang M, Li Y. Engineered macrophage membrane-enveloped nanomedicine for ameliorating myocardial infarction in a mouse model. *Bioeng Transl Med*. 2021;6:e10197. https://doi.org/10.1002/btm2.10197